

# Conical ultrashort echo time (UTE) MRI in the evaluation of pediatric acute appendicitis

Albert T. Roh,<sup>1</sup> Zhibo Xiao,<sup>2</sup> Joseph Y. Cheng,<sup>1</sup> Shreyas S. Vasanaawala,<sup>1</sup> and Andreas M. Loening<sup>1</sup>

<sup>1</sup>Radiology, Stanford University, 300 Pasteur Drive, Stanford, CA 94305, USA

<sup>2</sup>Radiology, First Affiliated Hospital, Chongqing, China

## Abstract

**Purpose:** Magnetic resonance imaging (MRI) sequences with conical  $k$ -space trajectories are able to decrease motion artifacts while achieving ultrashort echo times (UTE). We assessed the performance of free-breathing conical UTE MRI in the evaluation of the pediatric pelvis for suspected appendicitis.

**Methods:** Our retrospective review of 84 pediatric patients who underwent MRI for suspected appendicitis compared three contrast-enhanced sequences: free-breathing conical UTE, breath-hold three-dimensional (3D) spoiled gradient echo (BH-SPGR), and free-breathing high-resolution 3D SPGR (FB-SPGR). Two radiologists performed blinded and independent evaluations of each sequence for image quality (four point scale), anatomic delineation (four point scale), and diagnostic confidence (five point scale). Subsequently, the three sequences were directly compared for overall image quality (−3 to +3 scale). Scores were compared using Kruskal–Wallis and Wilcoxon signed-rank tests.

**Results:** UTE demonstrated significantly better perceived signal-to-noise ratio (SNR) and fewer artifacts than BH-SPGR and FB-SPGR (means of 3.6 and 3.4, 3.4 and 3.2, 3.1 and 2.7, respectively;  $p < 0.0006$ ). BH-SPGR and FB-SPGR demonstrated significantly better contrast than UTE (means of 3.6, 3.4, and 3.2, respectively;  $p < 0.03$ ). In the remaining categories, UTE performed significantly better than FB-SPGR ( $p < 0.00001$ ), while there was no statistical difference between UTE and BH-SPGR. Direct paired comparisons of overall image quality demonstrated the readers significantly preferred UTE over both BH-SPGR (mean + 0.5,  $p < 0.00001$ ) and FB-SPGR (mean + 1.2,  $p < 0.00001$ ).

**Conclusions:** In the evaluation of suspected appendicitis, free-breathing conical UTE MRI performed better in the assessed metrics than FB-SPGR. When compared to BH-SPGR, UTE demonstrated superior perceived SNR and fewer artifacts.

**Key words:** Ultrashort echo time—Non-Cartesian—Pediatric—Appendicitis—Pelvis

Acute appendicitis is a common condition that requires emergent treatment, but the clinical presentation can be nonspecific and often requires imaging to confirm the diagnosis. Currently, ultrasound is a common first-line imaging modality to evaluate suspected acute appendicitis. However, not all hospitals have 24-h ultrasound technologist coverage, and ultrasound can be non-diagnostic in a large fraction of patients requiring the use of other imaging modalities to visualize the appendix and confirm the diagnosis [1–4]. Computed tomography (CT) is frequently used, as it is fast, readily available, and effective at diagnosing acute appendicitis. However, the ionizing radiation of CT is of concern, particularly for its use in children [5–12].

To reduce patient exposure to the ionizing radiation of CT, hospitals are increasingly using magnetic resonance imaging (MRI) either following non-diagnostic ultrasound examinations or as the initial diagnostic modality for appendicitis. MRI has no ionizing radiation and is effective at diagnosing acute appendicitis [13–17]. A limitation of MRI is its longer acquisition time compared to CT. Longer acquisition times may degrade image quality due to increased respiratory motion artifact and patient inability to cooperate, especially in the pediatric population. A focused protocol with only high-yield T2-weighted and contrast-enhanced sequences can reduce the exam time to less than 20 min [17]. Even with

Albert T. Roh and Zhibo Xiao contributed equally to this work and are considered co-first authors.

Correspondence to: Andreas M. Loening; email: [loening@stanford.edu](mailto:loening@stanford.edu)

this abbreviated protocol, motion artifacts remain a consideration when imaging children with suspected acute appendicitis.

Recent advancements in non-Cartesian MRI are useful in overcoming the limitations of respiratory and bowel motion in contrast-enhanced sequences. Newer techniques with conical  $k$ -space sampling trajectories are able to diffuse motion artifacts, decreasing blurring and increasing robustness to motion [18, 19]. Further, the conical trajectories have increased scan efficiency compared to three-dimensional (3D) pure radial acquisitions while maintaining the ability to achieve ultrashort echo times (UTE). UTE minimizes susceptibility artifacts from bowel gas, an important feature in abdominal imaging. These advantages potentially allow conical UTE to yield diagnostic images during free breathing, obviating the need for patients to cooperate with breath holds [20–24].

This study assessed contrast-enhanced conical UTE acquired during free breathing in the evaluation of the pediatric pelvis for suspected acute appendicitis. We hypothesized that this sequence could yield superior image quality to a breath-hold 3D dual-echo spoiled gradient echo (SPGR) sequence and a free-breathing high-resolution 3D SPGR sequence.

## Materials and methods

Our retrospective review was approved by the Institutional Review Board (IRB) with waiver of informed consent. Ninety pediatric patients (under the age of 18 years) who underwent contrast-enhanced MRI of the abdomen and pelvis for suspected acute appendicitis from November 2016 to October 2017 (1 year) were retrospectively identified. Six patients with incomplete exams that did not include all three sequences of interest were excluded; 84 patients were included in our study.

All exams were performed in a 3 T clinical MRI system (MR750w, GE Healthcare, Waukesha, Wisconsin) after the administration of intravenous contrast: 1.0 M gadobutrol at 0.1 mmol/kg (Gadavist, Bayer, Whippany, New Jersey). No oral contrast, bowel mobility inhibitor, or sedation was administered. In addition to T2-weighted and diffusion-weighted imaging sequences, each patient at our institution routinely undergoes three contrast-enhanced MRI sequences of the pelvis acquired in the axial plane (sequence parameters in Table 1):

- *UTE* free-breathing UTE ( $T_E$  of 0.03 ms) spoiled gradient echo (SPGR) without acceleration and using intermittent fat suppression. Data were acquired using a 3D conical  $k$ -space sampling trajectory. Each cone interleaf was ordered by the final  $k_z$  position. To increase motion robustness, each readout was then reordered using golden-ratio permutation [19]. No additional motion compensation was used; image artifacts were effectively reduced through averaging.

Note that the intermittent fat suppression pulse was used less frequently than in FB-SPGR to decrease scan time.

- *BH-SPGR* 3D SPGR with dual-echo water–fat separation (LAVA-Flex) utilizing parallel-imaging acceleration acquired during an attempted breath hold.
- *FB-SPGR* free-breathing high-resolution 3D SPGR without acceleration and using intermittent fat suppression.

Of the three contrast-enhanced sequences, BH-SPGR was performed first on all patients, followed by FB-SPGR then UTE in 69 patients (82%) and UTE then FB-SPGR in 15 patients (18%).

For each patient, age, gender, radiologic diagnosis, and clinical diagnosis were recorded. Radiologic diagnosis from the clinical radiology report was used and was not reassessed retrospectively; the clinical radiologist had access to all three sequences as well as additional T2-weighted and diffusion-weighted sequences. Clinical diagnosis in patients who underwent appendectomy was established from the operative and pathology reports. Clinical diagnosis was otherwise established by a 30-day chart review.

The primary outcomes of our study were to assess the image quality of conical UTE in the evaluation of the pediatric pelvis for suspected acute appendicitis, and to compare the performance of UTE to that of BH-SPGR and FB-SPGR. Two radiologists (ZX is a board-certified radiologist with 12 years of experience and ATR is a board-eligible radiology fellow with 4 years of experience) performed independent evaluations on a Likert scale of each contrast-enhanced sequence in the axial plane for image quality, anatomic delineation, and diagnostic confidence. The readers reviewed each sequence independently, blinded to the other sequences of each patient, with patients and sequences presented in a randomized order. Prior to this assessment, an instructional tutorial was provided to the readers, including typical cases and suggested data scores for these data sets. Image quality features included subjective assessments of signal-to-noise ratio (SNR), contrast, presence of artifacts (e.g., coherent motion artifacts, field inhomogeneity), and blurring. They were scored on a 1–4 scale with 1 representing non-diagnostic images, 2 representing images considered of limited diagnostic value, 3 representing sub-par images but still of diagnostic quality, and 4 representing excellent diagnostic quality. Anatomic delineation of the appendix, small bowel, colon, and bladder was assessed similarly on a 1–4 scale. Diagnostic confidence in the ability to diagnose or exclude appendicitis was scored from 1 to 5 (low to high confidence).

Subsequently, in a separate session after a time interval of at least 1 week to minimize recall bias, the three sequences were reevaluated for overall image quality and directly compared to each other with paired

**Table 1.** MRI scan parameters

Parameters	UTE	BH-SPGR	FB-SPGR
$T_R$ (ms)	4.7	4.1	4.7
$T_E$ (ms)	0.03	1.1/2.2	1.1
Bandwidth (kHz)	125	166.7	62.5
Field of view (cm)	40	34	40
Matrix	416 × 416 × 284	320 × 256 × 152	512 × 512 × 292
Slice thickness (mm)	1.4	3	1.4
Flip angle (°)	15	15	15
Scan time (min)	5:09	0:16	5:03
Acceleration	None	Phase direction: 2.0 Slice direction: 1.5	None

Note that slice spacing in all three sequences was reduced by 50% compared to the slice thickness through interpolation during reconstruction

**Table 2.** Comparison of perceived image quality, anatomic delineation, and diagnostic confidence

Assessment	Features	Mean score			Kruskal–Wallis test $p$ values	Wilcoxon signed-rank test $p$ values	
		UTE	BH-SPGR	FB-SPGR		UTE ≠ BH-SPGR	UTE ≠ FB-SPGR
Image quality	Perceived SNR	3.6	3.4	3.1	<i>0.00001</i>	<i>0.00001</i>	<i>0.00001</i>
	Contrast	3.2	3.6	3.4	<i>0.00098</i>	<i>0.00001</i>	<i>0.03236</i>
	Artifacts	3.4	3.2	2.7	<i>0.00001</i>	<i>0.00064</i>	<i>0.00001</i>
	Blurring	3.2	3.0	2.6	<i>0.00001</i>	0.09894	<i>0.00001</i>
Anatomic delineation	Appendix	3.0	2.9	2.4	<i>0.00001</i>	0.06432	<i>0.00001</i>
	Small bowel	3.1	2.9	2.4	<i>0.00001</i>	0.02926	<i>0.00001</i>
	Colon	3.5	3.3	2.8	<i>0.00001</i>	0.02510	<i>0.00001</i>
	Bladder	3.7	3.6	3.3	<i>0.00010</i>	0.04884	<i>0.00001</i>
Diagnostic confidence		4.0	3.8	3.2	<i>0.00001</i>	0.01314	<i>0.00001</i>

Italics denote statistical significance after a Bonferroni–Holm multiple comparisons correction

simultaneous viewing in blinded and randomized order (scored between  $-3$  and  $+3$ ; inferior to superior). A score of 0 indicated similar image quality, a score of  $-1$  or  $+1$  indicated aesthetically improved image quality, a score of  $-2$  or  $+2$  indicated improved diagnostic quality, and a score of  $-3$  or  $+3$  indicated better structural delineation, with negative scores favoring the image presented on the right. Scores were transposed appropriately after unblinding so that positive scores favored UTE, and negative scores favored BH-SPGR and FB-SPGR.

The reader scores for each sequence were pooled. The three sequences were compared simultaneously using a Kruskal–Wallis test, followed by paired comparisons between each set of sequences using a Wilcoxon signed-rank test. Wilcoxon signed-rank test was performed to assess for a difference from zero in the direct paired comparisons of the three sequences to each other. Subgroup analysis using Wilcoxon rank-sum test was performed comparing the patients with UTE performed before FB-SPGR to those with UTE after FB-SPGR. An additional subgroup analysis using Wilcoxon rank-sum test was performed comparing the younger patients with age of 8 years and under (22 patients, 26%) to the older patients over the age of 8 years (62 patients, 74%). Kruskal–Wallis and Wilcoxon signed-rank tests were again performed on the younger cohort to compare the three sequences. For all tests, statistical significance was set to achieve a  $p$  value  $< 0.05$ , decreased as needed for

multiple comparisons using a Bonferroni–Holm correction. Inter-observer agreement was evaluated with intraclass correlation coefficient (ICC). ICC values  $< 0.40$  corresponded to poor agreement, 0.40–0.59 to fair, 0.60–0.74 to good, and  $> 0.75$  to excellent.

## Results

The mean age of the subjects was 11 years, ranging from 2 to 18 years; 56% of subjects (47 out of 84) were female. The appendix was visualized in 63 patients (75%). Of the 84 included patients, 14 (17%) were diagnosed with acute appendicitis and 23 (27%) with alternative diagnoses [including 7 (8%) with right ovarian etiologies, 7 (8%) with mesenteric adenitis, 5 (6%) with gastrointestinal etiologies, and 2 (2%) with urinary tract etiologies].

UTE demonstrated significantly better perceived SNR and fewer artifacts (Table 2) than both BH-SPGR and FB-SPGR ( $p < 0.0006$ ); both BH-SPGR and FB-SPGR demonstrated significantly better contrast ( $p < 0.03$ ) than UTE. Representative examples are shown in Figs. 1, 2 and 3. After correcting for multiple comparisons, there was no statistical difference between UTE and BH-SPGR in blurring, anatomic delineation, and diagnostic confidence ( $p > 0.013$ ). Other than contrast, UTE performed better than FB-SPGR in the remaining categories ( $p < 0.00001$ ). Direct paired comparisons of overall image quality demonstrated similar results (Table 3): the readers significantly preferred UTE

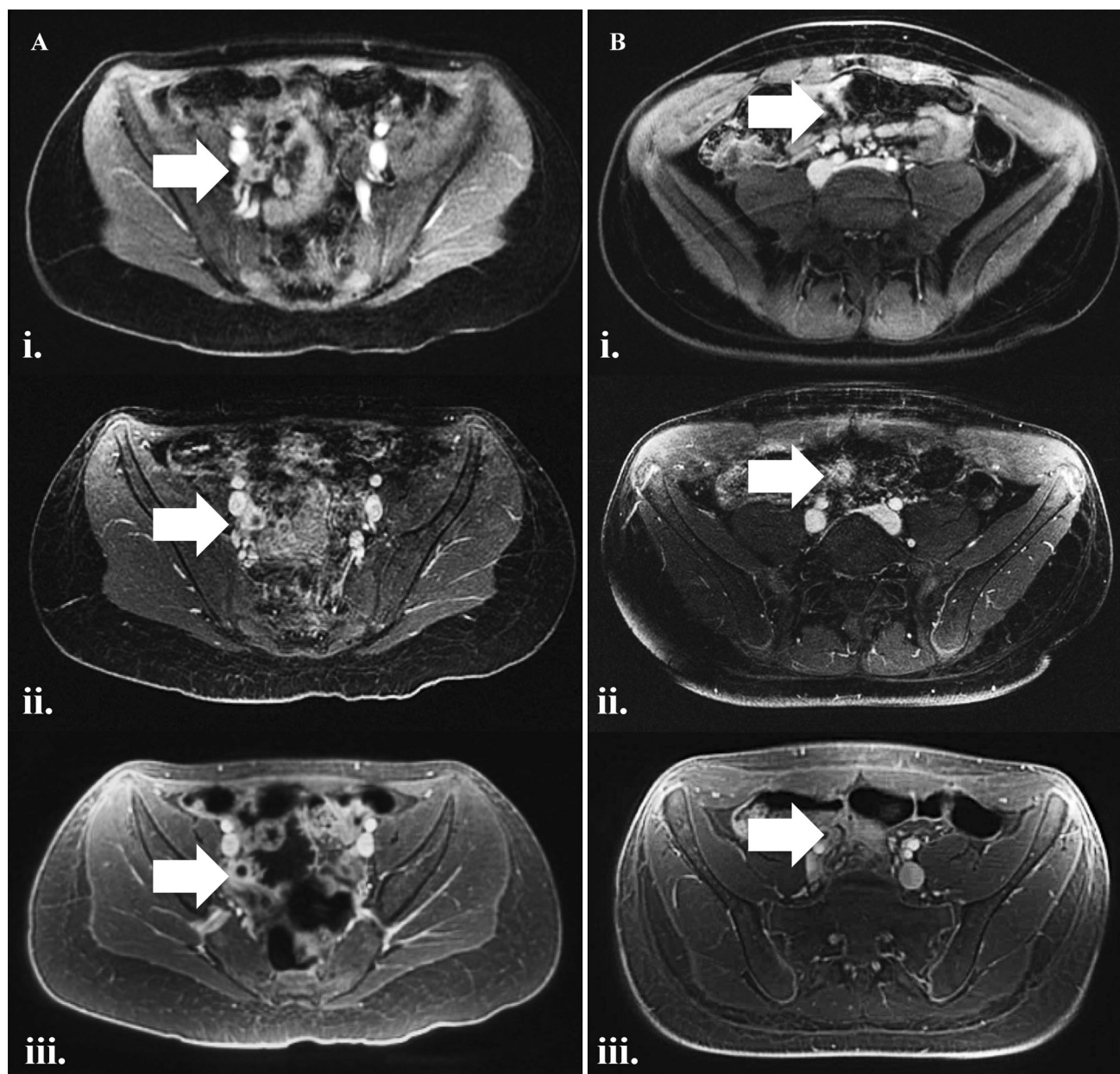


**Fig. 1.** Two representative cases of **A** acute appendicitis and **B** normal appendix labeled on each sequence with white arrows. Note reduced bowel gas related field inhomogeneity artifact and decreased respiratory motion artifact on UTE. Also note that fat signal on UTE is appreciably brighter than

on FB-SPGR; this is a sequela of the intermittent fat suppression pulse being applied less frequently in an effort to reduce scan time. (i) BH-SPGR, (ii) FB-SPGR and (iii) UTE.

over both BH-SPGR and FB-SPGR (means of + 0.5 and + 1.2, respectively;  $p < 0.00001$ ).

Subgroup analysis comparing the patients with UTE performed before FB-SPGR to those with UTE after FB-SPGR determined that FB-SPGR yielded better contrast, anatomic delineation of colon and bladder, and fewer artifacts ( $p < 0.002$ ) when performed before UTE compared to FB-SPGR performed after UTE (Table 4). There was no statistical signifi-

cance in any category for UTE when performed before FB-SPGR compared to UTE performed after FB-SPGR.

Subgroup analysis comparing the younger patients with age of 8 years and under to the older patients over the age of 8 years (Table 5) demonstrated better image quality, anatomic delineation, and diagnostic confidence in all three sequences in the older cohort ( $p < 0.02$ ). Comparison of the three sequences in the 22 patients in

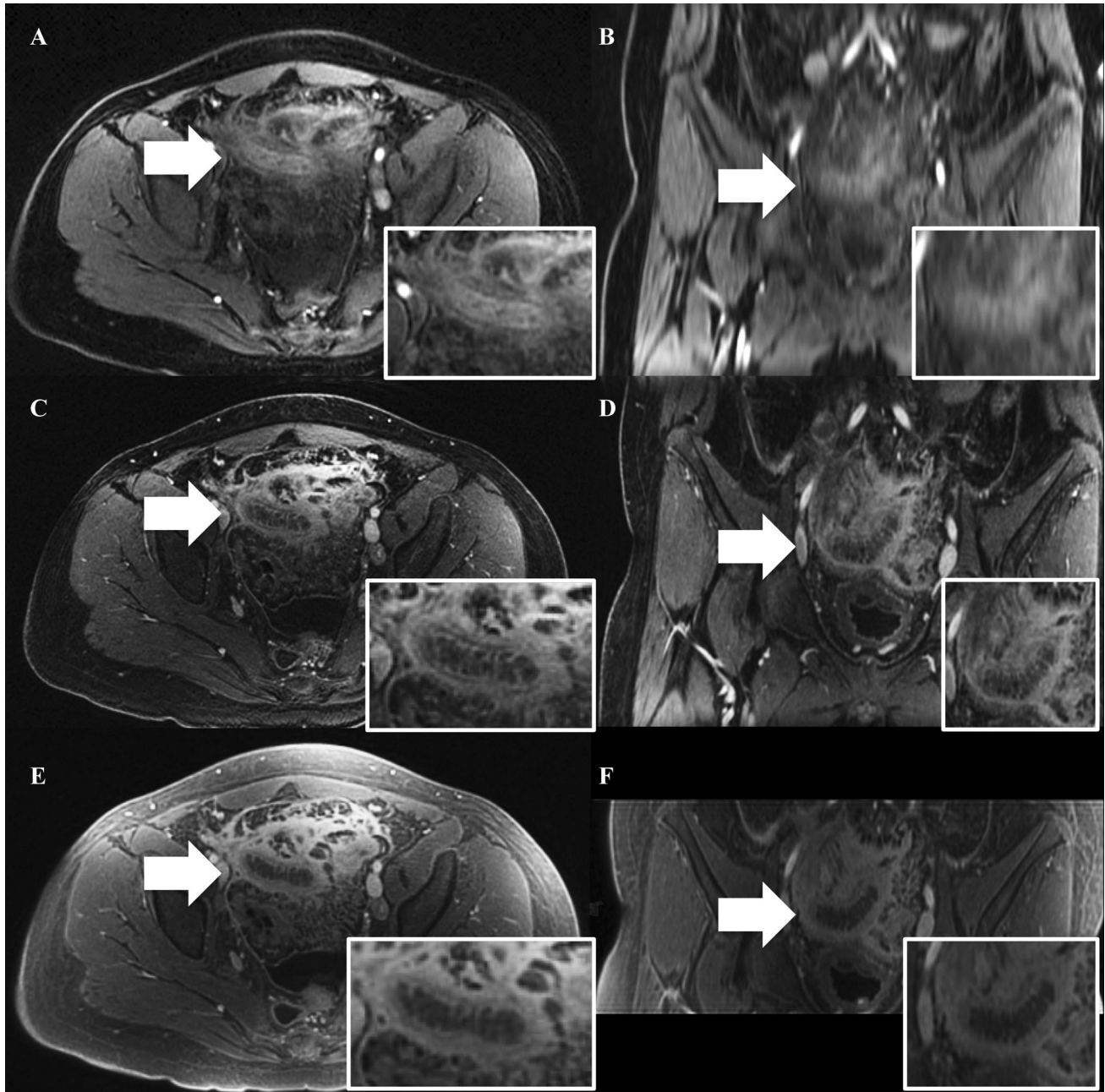


**Fig. 2.** A representative case of acute appendicitis labeled on each sequence with white arrows. Note the improved image quality of the coronal reconstructions on FB-SPGR and UTE. **A** BH-SPGR in the axial plane, **B** BH-SPGR in the

coronal plane, **C** FB-SPGR in the axial plane, **D** FB-SPGR in the coronal plane, **E** UTE in the axial plane, and **F** UTE in the coronal plane.

the younger cohort only (Table 6) demonstrated significantly better perceived SNR, appendix anatomic delineation, and diagnostic confidence with UTE when compared to BH-SPGR ( $p < 0.007$ ). Other than contrast (which demonstrated no statistical significance), UTE performed statistically better than FB-SPGR in all other categories ( $p < 0.0001$ ).

Inter-observer agreement in ratings was greater overall for UTE and BH-SPGR than FB-SPGR

(Table 7). Both UTE and BH-SPGR had six (out of nine) parameters with good to excellent inter-observer agreement ( $ICC > 0.60$ ), compared to FB-SPGR with four.

## Discussion

In our study, we demonstrated the feasibility and high image quality of free-breathing conical UTE MRI of the pediatric pelvis in the evaluation of suspected acute

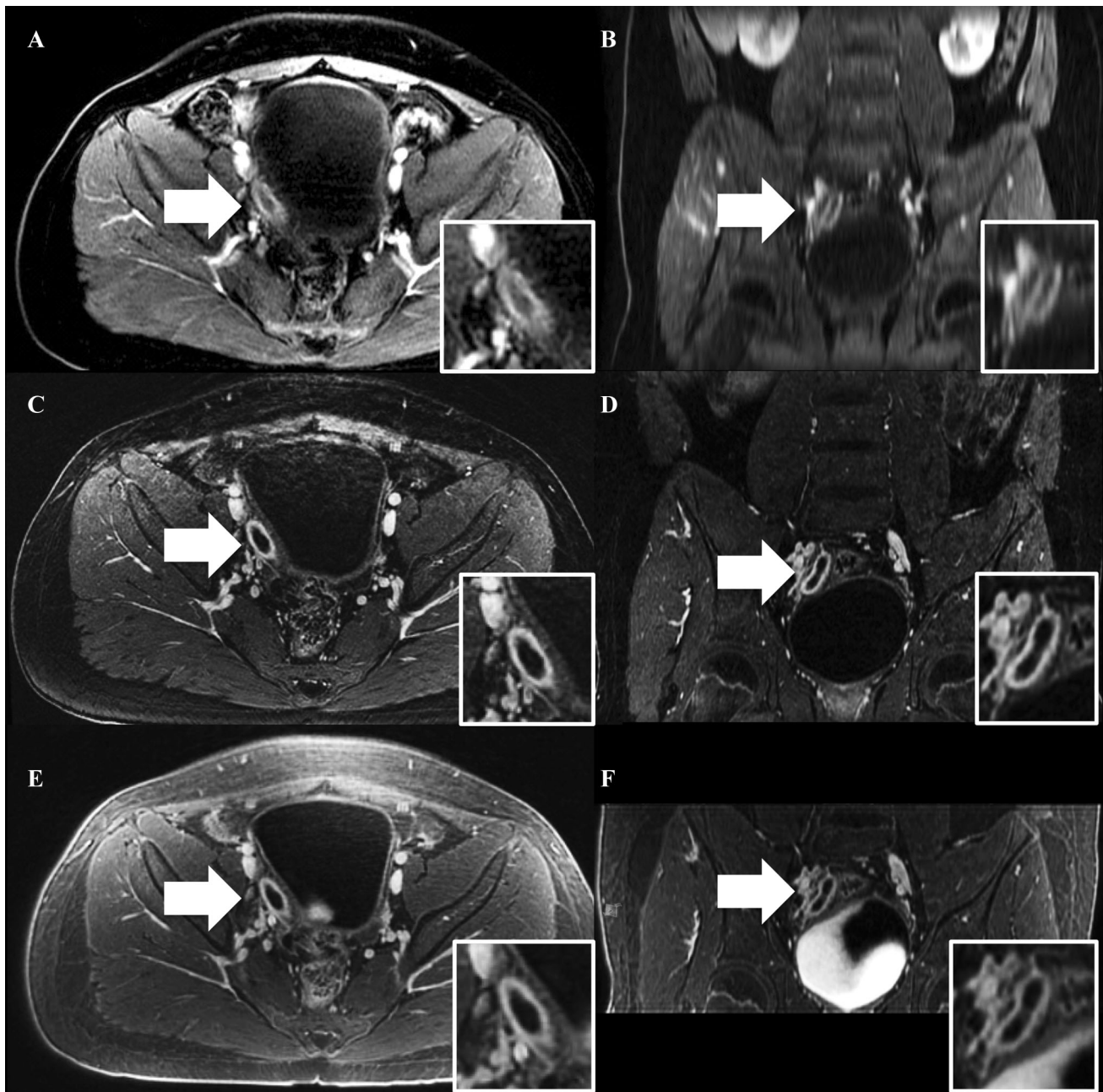


**Fig. 3.** A representative case of acute appendicitis labeled on each sequence with white arrows. Note the improved image quality of the coronal reconstructions on FB-SPGR and UTE. **A** BH-SPGR in the axial plane, **B** BH-SPGR in the

coronal plane, **C** FB-SPGR in the axial plane, **D** FB-SPGR in the coronal plane, **E** UTE in the axial plane, and **F** UTE in the coronal plane.

appendicitis. Other than for contrast, UTE performed better than and was preferred by our readers over the comparison free-breathing sequence, FB-SPGR. When compared to the breath-hold sequence (BH-SPGR), UTE demonstrated superior perceived SNR and fewer artifacts (Fig. 1), but again had inferior contrast. To decrease scan time, we used an intermittent fat suppression pulse with less fat suppression than the other sequences, which may explain in part the inferior contrast

rating by the readers. Despite the inferior perceived image contrast, the readers still preferred the overall image quality of UTE over that of BH-SPGR.

The primary disadvantage of UTE in comparison to BH-SPGR was scan time (5:09 for UTE and 0:16 for BH-SPGR). However, the tradeoff for the shorter scan time with BH-SPGR was the need for acceleration, decreased spatial resolution in all three planes, and the need for patient cooperation with breath hold instructions. These

**Table 3.** Direct paired comparisons of overall image quality

	Mean scores	<i>p</i> values	ICC
UTE vs. BH-SPGR	+ 0.5	<i>0.00001</i>	<i>0.65</i>
UTE vs. FB-SPGR	+ 1.2	<i>0.00001</i>	<i>0.68</i>

Positive scores favor the first of the listed sequences; negative scores favor the second. Italics denote statistical significance (*p* values < 0.05) and good to excellent inter-observer agreement (ICC > 0.60)

compromises manifested themselves as the inferior perceived SNR and increased artifacts in BH-SPGR. Also, although the image quality of multiplanar reconstructions was not assessed in our study, it would be expected that UTE (and FB-SPGR) would be more amenable to reformatting due to the thinner acquired slice thicknesses (Figs. 2, 3).

**Table 4.** Subgroup analysis comparing the patients with FB-SPGR performed before UTE (69 patients) to those with FB-SPGR performed after UTE (15 patients)

Assessment	Features	FB-SPGR mean scores		<i>p</i> values	UTE mean scores		<i>p</i> values
		Before UTE	After UTE		Before FB-SPGR	After FB-SPGR	
Image quality	Perceived SNR	3.4	3.1	<i>0.0109</i>	3.7	3.5	0.6487
	Contrast	3.8	3.3	<i>0.0012</i>	3.3	2.9	0.0666
	Artifacts	3.1	2.6	<i>0.0022</i>	3.6	3.4	0.0669
	Blurring	2.7	2.6	<i>0.3755</i>	3.2	3.1	0.5761
Anatomic delineation	Appendix	2.9	2.4	<i>0.0292</i>	3.2	3.0	0.5277
	Small bowel	2.8	2.3	<i>0.0156</i>	3.1	2.9	0.1935
	Colon	3.4	2.7	<i>0.0003</i>	3.6	3.5	0.7751
	Bladder	3.8	3.2	<i>0.0010</i>	3.8	3.7	0.3867
Diagnostic confidence		3.7	3.1	<i>0.0288</i>	4.1	4.0	0.4289

Italics denote statistical significance after a Bonferroni–Holm multiple comparisons correction

**Table 5.** Subgroup analysis comparing the younger patients with age of 8 years and under (22 patients) to older patients over the age of 8 years (62 patients)

Assessment	Features	UTE mean scores		<i>p</i> values	BH-SPGR mean scores		<i>p</i> values	FB-SPGR mean scores		<i>p</i> values
		Under 8	Over 8		Under 8	Over 8		Under 8	Over 8	
Image quality	Perceived SNR	3.4	3.8	<i>0.0014</i>	3.0	3.5	<i>0.00001</i>	2.7	3.3	<i>0.00001</i>
	Contrast	2.9	3.3	<i>0.0166</i>	3.2	3.7	<i>0.00001</i>	2.8	3.5	<i>0.00001</i>
	Artifacts	2.8	3.6	<i>0.00001</i>	2.6	3.4	<i>0.00001</i>	2.3	2.9	<i>0.0001</i>
	Blurring	2.8	3.3	<i>0.0001</i>	2.6	3.2	<i>0.00001</i>	2.1	2.8	<i>0.00001</i>
Anatomic delineation	Appendix	2.6	3.2	<i>0.0003</i>	2.1	3.2	<i>0.00001</i>	1.8	2.7	<i>0.00001</i>
	Small bowel	2.6	3.2	<i>0.0002</i>	2.4	3.1	<i>0.00001</i>	2.0	2.5	<i>0.0005</i>
	Colon	3.0	3.7	<i>0.00001</i>	2.6	3.6	<i>0.00001</i>	2.3	3.0	<i>0.0001</i>
	Bladder	3.3	3.8	<i>0.0013</i>	3.1	3.7	<i>0.0004</i>	2.7	3.5	<i>0.00001</i>
Diagnostic confidence		3.4	4.3	<i>0.00001</i>	2.9	4.1	<i>0.00001</i>	2.5	3.5	<i>0.00001</i>

Italics denote statistical significance after a Bonferroni–Holm multiple comparisons correction

**Table 6.** Comparison of perceived image quality, anatomic delineation, and diagnostic confidence of the subgroup of the younger patients with age of 8 years and under (22 patients)

Assessment	Features	Mean scores			Kruskal–Wallis test <i>p</i> values	Wilcoxon signed-rank test <i>p</i> values	
		UTE	BH-SPGR	FB-SPGR		UTE ≠ BH-SPGR	UTE ≠ FB-SPGR
Image quality	Perceived SNR	3.4	3.0	2.7	<i>0.00014</i>	<i>0.00164</i>	<i>0.00001</i>
	Contrast	2.9	3.2	2.8	0.17911	0.12356	0.53526
	Artifacts	2.8	2.6	2.3	<i>0.0082</i>	0.05	<i>0.0001</i>
	Blurring	2.8	2.6	2.1	<i>0.00099</i>	0.11184	<i>0.00001</i>
Anatomic delineation	Appendix	2.6	2.1	1.8	<i>0.00055</i>	<i>0.002</i>	<i>0.00001</i>
	Small bowel	2.6	2.4	2.0	<i>0.00581</i>	0.05	<i>0.00001</i>
	Colon	3.0	2.6	2.3	<i>0.00284</i>	0.01078	<i>0.00001</i>
	Bladder	3.3	3.1	2.7	<i>0.02293</i>	0.16758	<i>0.00001</i>
Diagnostic confidence		3.4	2.9	2.5	<i>0.0007</i>	<i>0.00652</i>	<i>0.00008</i>

Italics denote statistical significance after a Bonferroni–Holm multiple comparisons correction

**Table 7.** Inter-observer agreement

Assessment	Features	ICC		
		UTE	BH-SPGR	FB-SPGR
Image quality	Perceived SNR	<i>0.90</i>	<i>0.82</i>	<i>0.73</i>
	Contrast	<i>0.54</i>	<i>0.79</i>	<i>0.74</i>
	Artifacts	<i>0.85</i>	<i>0.75</i>	<i>0.65</i>
	Blurring	<i>0.83</i>	<i>0.64</i>	<i>0.50</i>
Anatomic delineation	Appendix	<i>0.39</i>	<i>0.59</i>	<i>0.57</i>
	Small bowel	<i>0.68</i>	<i>0.45</i>	<i>0.59</i>
	Colon	<i>0.49</i>	<i>0.64</i>	<i>0.60</i>
	Bladder	<i>0.75</i>	<i>0.68</i>	<i>0.48</i>
Diagnostic confidence		<i>0.66</i>	<i>0.56</i>	<i>0.57</i>

Italics denote good to excellent inter-observer agreement (ICC > 0.60)

In addition, image acquisition during free breathing (with UTE and FB-SPGR) instead of during an attempted breath hold (with BH-SPGR) may serve as an advantage in patients unable to cooperate with breath hold instructions, such as younger patients and those in significant pain. In certain circumstances, 5 min of free breathing may be more feasible than a 16 s breath hold, favoring UTE (and FB-SPGR) over BH-SPGR. In our younger cohort with age of 8 years and under, the readers scored UTE higher for appendix anatomic delineation and diagnostic confidence when compared to BH-SPGR, differences that were not apparent in the overall patient population; these additional benefits highlight UTE's potential value in younger patients. UTE can also be used as a troubleshooting/salvage sequence in patients with significant respiratory motion artifact demonstrated on BH-SPGR. UTE can be further improved through motion compensation such as soft-gating [19], and acquisition time could be decreased with the implementation of acceleration techniques.

To the best of our knowledge, there are no prior studies evaluating UTE in the pelvis. Current uses of UTE predominate in musculoskeletal MRI due to its ability to image structures with short T2 properties, such as cortical bone and fibrocartilage [25–27]. UTE has also demonstrated value in the head, chest, and liver [19, 28–30]. While the applications in the head similarly take advantage of the ability of UTE to image cortical bone, its value in the chest and liver are based on its robustness to motion. Our study establishes that UTE is feasible in the evaluation of the pediatric pelvis for suspected acute appendicitis and any mimicking acute pelvic pathology, with advantages over both BH-SPGR and FB-SPGR, which may be due to decreased motion artifact.

UTE demonstrated anatomic delineation of the bladder, small bowel, and colon (in addition to the appendix) that was comparable to that of BH-SPGR and superior to that of FB-SPGR. UTE's superior anatomic delineation compared to FB-SPGR may in part be due to UTE's decreased susceptibility to bowel gas artifacts and

motion robustness. Further research to assess UTE in the evaluation of pathology specific to these pelvic structures may be considered. For example, utilization of the ability of UTE to reformat its images in multiple planes may be beneficial in both colorectal and gynecologic cancer staging; future studies investigating these additional applications would be of interest. Also, given that it yields decreased motion artifact when compared to BH-SPGR and FB-SPGR, UTE may demonstrate value in the abdomen. Another consideration is to confirm our pediatric results in the adult population, although respiratory motion and patient cooperation may be of less concern in adults.

Limitations of our study include its unequal distribution of patients when timing the FB-SPGR and UTE sequences. FB-SPGR was performed before UTE in 82% of our patients; in subgroup analysis, this yielded better image quality and anatomic delineation during that earlier phase of contrast compared to when FB-SPGR was performed after UTE. Despite this disparity that biased the study towards FB-SPGR, our study rated UTE superior to FB-SPGR. BH-SPGR was performed first on all patients; however, given that it was only a 16-s sequence, any advantage from its earlier timing was considered negligible. Another limitation is the lack of true blinding; due to the unique appearance of each sequence, the sequence identity is usually apparent to the reader despite blinding and randomization. Also, the assessed metrics in our study were subjective to the readers and were not based on objective measurements such as signal-to-noise ratio, although this could potentially be considered a strength as it factors in human perception into the image evaluation process. Other limitations of our study are its retrospective study design and relatively small sample size. Prospective research is warranted to validate our results.

In summary, free-breathing conical UTE MRI of the pediatric pelvis in the evaluation of suspected acute appendicitis is feasible, yielding better perceived SNR and fewer artifacts than both BH- and FB-SPGR.

### Compliance with ethical standards

**Funding** This study was funded by NIBIB R01EB009690.

**Conflict of interest** Albert T. Roh, Zhibo Xiao, Joseph Y. Cheng, and Andreas M. Loening declare that they have no conflict of interest. Shreyas S. Vasanawala has received grant support from NIBIB R09EB009690.

**Ethical approval** All procedures performed in studies involving human participants were in accordance with the ethical standards of the Institutional Research Committee and with the 1964 Helsinki Declaration and its later amendments or comparable ethical standards.

### References

- Doria AS, Moineddin R, Kellenberger CJ, et al. (2006) US or CT for diagnosis of appendicitis in children and adults? A meta-analysis. *Radiology* 241:83–94
- Garcia Pena BM, Mandl KD, Kraus SJ, et al. (1999) Ultrasonography and limited computed tomography in the diagnosis and management of appendicitis in children. *JAMA* 282:1041–1046
- Rothrock SG, Pagane J (2000) Acute appendicitis in children: emergency department diagnosis and management. *Ann Emerg Med* 36:39–51
- Wan MJ, Krahn M, Ungar WJ, et al. (2009) Acute appendicitis in young children: cost-effectiveness of US versus CT in diagnosis—a Markov decision analytic model. *Radiology* 250:378–386
- Brenner DJ, Hall EJ (2007) Computed tomography—an increasing source of radiation exposure. *N Engl J Med* 357:2277–2284
- Brody AS, Frush DP, Huda W, et al. (2007) Radiation risk to children from computed tomography. *Pediatrics* 120:677–682
- Callahan MJ (2011) CT dose reduction in practice. *Pediatr Radiol* 41:488–492
- Macdougall RD, Strauss KJ, Lee EY (2013) Managing radiation dose from thoracic multidetector computed tomography in pediatric patients: background, current issues, and recommendations. *Radiol Clin N Am* 51:743–760
- Pearce MS, Salotti JA, Little MP, et al. (2012) Radiation exposure from CT scans in childhood and subsequent risk of leukaemia and brain tumours: a retrospective cohort study. *Lancet* 380:499–505
- Sivit CJ, Applegate KE, Berlin SC, et al. (2000) Evaluation of suspected appendicitis in children and young adults: helical CT. *Radiology* 216:430–433
- Slovic TL, Berdon WE (2002) The ALARA concept in pediatric CT intelligent dose reduction. *Pediatr Radiol* 32:217–317
- Verdun FR, Bochud F, Gudinchet F, et al. (2008) Quality initiatives radiation risk: what you should know to tell your patient. *RadioGraphics* 28:1807–1816
- Duke E, Kalb B, Arif-Tiwari H, et al. (2016) A systematic review and meta-analysis of diagnostic performance of MRI for evaluation of acute appendicitis. *AJR* 206(3):508–517
- Johnson AK, Filippi CG, Andrews T, et al. (2012) Ultrafast 3-T MRI in the evaluation of children with acute lower abdominal pain for the detection of appendicitis. *AJR* 198:1424–1430
- Moore MM, Gustas CN, Choudhary AK, et al. (2012) MRI for clinically suspected pediatric appendicitis: an implemented program. *Pediatr Radiol* 42:1056–1063
- Rosines LA, Chow DS, Lampl BS, et al. (2014) Value of gadolinium-enhanced MRI in detection of acute appendicitis in children and adolescents. *AJR* 203(5):543–548
- Koning JL, Naheed JH, Kruk PG (2014) Diagnostic performance of contrast-enhanced MR for acute appendicitis and alternative causes of abdominal pain in children. *Pediatr Radiol* 44:948–955
- Gurney PT, Hargreaves BA, Nishimura DG (2006) Design and analysis of a practical 3D cones trajectory. *Magn Reson Med* 55(3):575–582
- Zucker EJ, Cheng JY, Haldipur A, et al. (2018) Free-breathing pediatric chest MRI: performance of self-navigated golden-angle ordered conical ultrashort echo time acquisition. *J Magn Reson Imaging* 47:200–209
- Carl M, Bydder GM, Du J (2016) UTE imaging with simultaneous water and fat signal suppression using a time-efficient multispoke inversion recovery pulse sequence. *Magn Reson Med* 55:575–582
- Kazantsev IG, Matej S, Lewitt RM (2005) Optimal ordering of projections using permutation matrices and angles between projection subspaces. *Electron Notes Discret Math* 20:205–216
- Robison RK, Anderson AG III, Pipe JG (2016) Three-dimensional ultrashort echo-time imaging using a FLORET trajectory. *Magn Reson Med*. <https://doi.org/10.1002/mrm.26500>
- Winkelmann S, Schaeffter T, Koehler T, et al. (2007) An optimal radial profile order based on the golden ratio for time-resolved MRI. *IEEE Trans Med Imaging* 26:68–76
- Zhang T, Cheng JY, Chen Y, et al. (2016) Robust self-navigated body MRI using dense coil arrays. *Magn Reson Med* 76:197–205
- Chang EY, Du J, Chung CB (2015) UTE imaging in the musculoskeletal system. *J Magn Reson Imaging* 41(4):870–883
- Siriwanarangsun P, Statum S, Biswas R, et al. (2016) Ultrashort time to echo magnetic resonance techniques for the musculoskeletal system. *Quant Imaging Med Surg* 6(6):731–743
- Serai SD, Laor T, Dwek JR, et al. (2014) Feasibility of ultrashort TE (UTE) imaging of children at 1.5 T. *Pediatr Radiol* 44(1):103–108
- Shu SH, Cao Y, Lawrence TS, et al. (2015) Quantitative characterization of ultrashort echo (UTE) images for supporting air-bone separation in the head. *Phys Med Biol* 60(7):2869–2880
- Ohno Y, Koyama H, Yoshikawa T, et al. (2016) Pulmonary high-resolution ultrashort TE MR imaging: comparison with thin-section standard- and low-dose computed tomography for the assessment of pulmonary parenchyma diseases. *J Magn Reson Imaging* 43(2):512–532
- Doyle EK, Toy K, Valdez B, et al. (2017) Ultra-short echo time images quantify high liver iron. *Magn Reson Med*. <https://doi.org/10.1002/mrm.26791>